

# Preliminary Results from a Heavily Instrumented Engine Ice Crystal Icing Test in a Ground Based Altitude Test Facility

Ashlie B. Flegel<sup>1</sup>

Michael J. Oliver<sup>2</sup>

*NASA Glenn Research Center, Cleveland, Ohio, 44135*

Preliminary results from the heavily instrumented ALF502R-5 engine test conducted in the NASA Glenn Research Center Propulsion Systems Laboratory are discussed. The effects of ice crystal icing on a full scale engine is examined and documented. This same model engine, serial number LF01, was used during the inaugural icing test in the Propulsion Systems Laboratory facility. The uncommanded reduction of thrust (rollback) events experienced by this engine in flight were simulated in the facility. Limited instrumentation was used to detect icing on the LF01 engine. Metal temperatures on the exit guide vanes and outer shroud and the load measurement were the only indicators of ice formation. The current study features a similar engine, serial number LF11, which is instrumented to characterize the cloud entering the engine, detect/characterize ice accretion, and visualize the ice accretion in the region of interest. Data were acquired at key LF01 test points and additional points that explored: icing threshold regions, low altitude, high altitude, spinner heat effects, and the influence of varying the facility and engine parameters. For each condition of interest, data were obtained from some selected variations of ice particle median volumetric diameter, total water content, fan speed, and ambient temperature. For several cases the NASA in-house engine icing risk assessment code was used to find conditions that would lead to a rollback event. This study further helped NASA develop necessary icing diagnostic instrumentation, expand the capabilities of the Propulsion Systems Laboratory, and generate a dataset that will be used to develop and validate in-house icing prediction and risk mitigation computational tools. The ice accretion on the outer shroud region was acquired by internal video cameras. The heavily instrumented engine showed good repeatability of icing responses when compared to the key LF01 test points and during day-to-day operation. Other noticeable observations are presented.

## Nomenclature

EGV	=	exit guide vane
IGV	=	inlet guide vane
MVD	=	median volumetric diameter [ $\mu\text{m}$ ]
$N1$	=	fan speed [rpm]
$N2$	=	compressor speed [rpm]
PLA	=	power lever angle [degree]
TWC	=	total water content [ $\text{g}/\text{m}^3$ ]

## I. Introduction

Developing a ground based altitude ice crystal icing simulation capability to conduct research on full scale engines and driven rigs is a key focus at NASA Glenn under the Aeronautics Evaluation and Test Capabilities (AETC) Project. In 2010, using the technology from the spray bar system in the Icing Research Tunnel (IRT), the Propulsion Systems Laboratory test cell 3 (PSL-3) was modified to enable icing research.<sup>1</sup> In 2013 the inaugural ice crystal icing test was conducted<sup>2</sup> on an unmodified ALF502R-5 engine, serial number LF01, which was used during Honeywell's 1997 flight test.<sup>3</sup> This inaugural test demonstrated PSL's capability by simulating key flight test points including several full rollbacks. By developing this icing capability in PSL, detailed datasets can be generated to help understand the underlying physics and validate engine icing prediction and simulations codes.<sup>4-7</sup> This modeling capability is one of the milestones of the Advanced Air Transport Technology (AATT) Project, which has

---

<sup>1</sup> Aerospace Research Engineer, Icing Branch, 21000 Brookpark Rd., Mail Stop 11-2, AIAA Member.

<sup>2</sup> Research Test Engineer, Wind Tunnel and Propulsion Test Branch, 21000 Brookpark Rd., Mail Stop 125-1, AIAA Member.

the goals of understanding the relevant icing physics associated with various types of known engine icing hazards, developing an engineering model and icing risk assessment tools to be available to the aviation community, and assessing the potential icing risks and ice protection system requirement for the N+2/ N+3 design concepts. No data exists in the open literature that experimentally examines the behavior and ice accretion in a full scale engine at altitude conditions. Previous fundamental tests have been conducted on a wedge and NACA 0012 airfoil shapes in an altitude tunnel in order to explore the local accretion mechanisms in mixed-phase conditions.<sup>8-10</sup> Through these experiments it has been found that local wet bulb temperature is critical to ice accretion or accumulation. Instrumentation is also being developed that can detect the ice without the need for internal engine cameras. The focus of the study presented in this paper is to further develop the PSL-3 icing test capability, improve instrumentation, and generate data to be used to assess ice crystal icing. This data will also augment the data from the previous PSL engine test that featured a similar engine with limited instrumentation.<sup>2</sup>

## II. Facility Description

This study was conducted in the NASA Glenn Research Center Propulsion Systems Laboratory Test Cell 3 (PSL-3), shown in Fig. 1. This facility has been used to conduct a wide variety of tests on turbofan, turboshaft, turbine-based combine cycle, and unmanned aerial vehicle engines for both commercial and military application since the early 1970's.<sup>1</sup> PSL-3 is a direct-connect altitude test chamber. The facility inlet air is provided by the NASA Central Process System (CPS) combustion air which delivers pressurized clean, dry, and ambient temperature air. The air passes through turbo expanders which cool the air and is then injected with steam. This fully-mixed steam-controlled air enters the plenum and passes through the icing spray bar grid where it is then injected with an icing cloud. The ice particles are formed by the rapid freeze-out of the water droplet cloud generated from the spray bar system. The tunnel walls are grounded in order to prevent the static cling of ice crystals on the wall. Once the air passes through the engine, the air is then exhausted into the chamber which is being pulled to 2.5 psia by the CPS altitude exhaust system. The facility conditions are set by adjusting the tunnel inlet pressure to achieve the desired Mach number and the exhaust pressure to maintain the altitude. The PSL-3 operating capabilities are shown in Table 1. When PSL-3 is configured for ice crystal icing tests the separate bypass airflow is closed off to prevent any potential ice buildup in the bypass duct. Therefore under icing configurations the facility has limited ability to simulate rapid throttle movements. Additional details of the facility and icing capability upgrades can be found in Soeder<sup>11</sup> and Griffin et.al.<sup>1</sup>

The cloud generation system is comprised of ten equally spaced spray bars with 222 nozzles, shown in Fig. 2. Two types of nozzles are featured on this system and they are the same type used in the NASA Icing Research Tunnel (IRT). The Standard nozzles are used for higher water content conditions. The Modified 1 (Mod. 1) nozzles are typically used for lower water content sprays. These nozzles are in a fixed, alternating pattern across each spray bar. Prior to each test entry the cloud is calibrated to the required condition subset and to understand the parameter space. The icing cloud operating envelope is shown in Fig. 3 and details of the PSL-3 cloud calibrations can be found in the following references.<sup>12,13</sup> PSL parameters that affect the cloud conditions include: altitude pressure, temperature, air mass flow rate, humidity, water type, and the following spray bar parameters: atomizing air pressure, water pressure, atomizing air temperature, water temperature, and cooling air temperature and pressure. For this current study, filtered non-demineralized city water was used to provide nucleation sites for the ice crystal development. During the inaugural ice crystal cloud calibration for the LF01 test, only the standard type nozzles were used.<sup>13</sup> During the LF01 test it was found that lower total water contents were needed. Having a better understanding of the required total water contents the Mod. 1 nozzles were used for this study in addition to the standard type nozzles. The cloud configurations with the nozzles were calibrated prior to this test.<sup>12</sup> Due to the nature of the facility transition duct, larger particles tend to concentrate toward the center of the duct. For this test the cloud was optimized by concentrating the nozzles to a circular area centered within the engine's projected splitter lip. The cloud calibration showed that the largest fully glaciated cloud MVD size achieved during this test was 85 $\mu$ m.

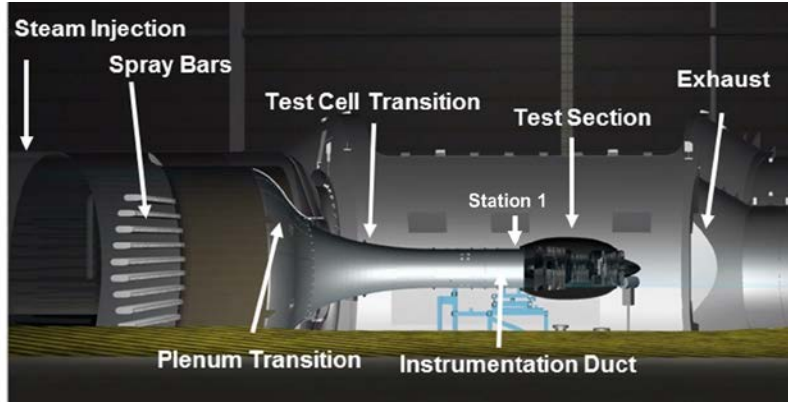


Figure 1. PSL-3 Facility Layout.

Table 1. PSL-3 Icing Configuration Operating Envelope.

Specification	Min	Max
Engine/ Rig Diameter, in.	24	72
Air Flow Rate, lb <sub>m</sub> /s	10	330
Altitude, kft	4	50
Total Temperature, °F	-60	50
Mach Number	0.15	0.80
TWC, g/m <sup>3</sup>	0.5	8.0*
MVD, μm	15	>100#

\* Evidence that probe under-measured

# Particles larger than ~ 90 microns are NOT fully glaciated

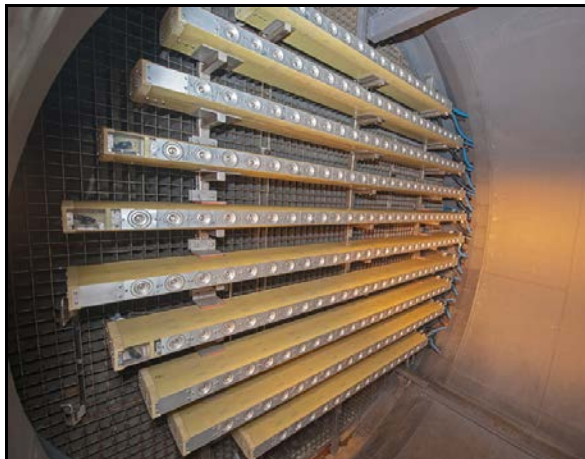


Figure 2. PSL-3 Spray Bar System.

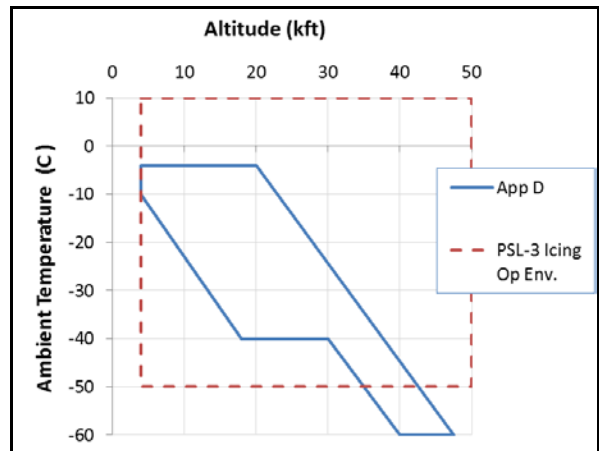


Figure 3. PSL-3 Icing Operating Envelope.

### III. Test Article Description

The engine used for this study was a heavily instrumented, unmodified ALF502R-5 engine, serial number LF11. This engine is the same model as the engine tested during the inaugural PSL engine icing test.<sup>3</sup> Details on the test article can be found in Table 2. The LF11 engine was instrumented with total pressure and total temperature probes along the leading edges of the stators of interest. Static pressure taps and thermocouples to acquire static pressure and metal surface temperatures were installed along the booster flow path, defined as the path between the entrance to the low pressure compressor and the entrance to the high pressure compressor, where ice crystal icing is theorized to occur in this test article. Further instrumentation details will be discussed later with additional engine instrumentation details described in Goodwin.<sup>14</sup> Like the LF01 engine, the spinner is heated and the IGVs have a

heated air anti-ice system. Two test days were conducted with an insulated spinner in order to investigate how the heated spinner influences possible accretion further downstream.

**Table 2. Engine Details<sup>3</sup>**

Parameter	Value
Bypass Ratio	5.7:1
Fan Diameter	40.25 in
Engine Length	64 in
Maximum Thrust	6970 lbf
Fan (# of stages)	1
Booster (# of stages)	1
Axial Compressor (# of stages)	7
Centrifugal HPC (# of stages)	1
High Pressure Turbine (# of stages)	2
Low Pressure Turbine (# of stages)	2

#### IV. Test Methodology

One of the goals during the engine tests is to develop test methodologies and procedures. The test methodologies developed during the LF01 testing were also used during the LF11 testing and are described below.

##### A. Facility Conditions

To set-up standard non-icing test conditions in PSL-3 which include plenum pressure ( $P_2$ ), temperature (TPL), and the test cell pressures respectively, the specification of a minimum of two flight simulation parameters are required:

1. The flight Mach number
2. The flight altitude.

For each icing test point conducted with an engine installed a calibration test point is performed with the engine not installed. This calibration procedure needs three additional cloud off parameters used to characterize the cloud calibration plane and the plenum total temperature with no engine installed:

1. The static temperature
2. The static pressure
3. The Mach number at engine inlet

These three parameters and cloud parameters, such as cloud *MVD* and *TWC*, from the calibration are then used to set-up the cloud conditions during an engine test with icing.

##### B. Cloud OFF and recovery procedures

A full engine roll back can expose the test article to a high risk of hardware damage due to the shedding of ice buildup in the flow path. In order to mitigate this risk, a called roll back procedure was developed.<sup>2</sup> The called roll back (CRB) procedure requires close monitoring of the measured load parameter, flow path static pressure, EGV metal temperatures, N1 and N2. Once a certain threshold of reduced measured load is met (7% of initial load for this study) accompanied by observed static pressure, temperature, N1 and N2 losses, a rollback is deemed imminent, the cloud is turned off and the engine is allowed to recover or return to initial cloud off operating condition.<sup>2</sup> Once the called rollback criteria is met the cloud is turned off and the PLA is reduced to recover the engine. If there is a heavy ice build the inlet humidity or plenum temperature is increased to melt the ice.

#### V. Instrumentation Description

The heavily instrumented ALF502R-5 engine, LF11, featured standard aero-research instrumentation along with advanced instrumentation to detect and characterize the ice. A cross section of the engine is shown in Fig. 4. The engine bypass was instrumented with total pressure and temperature probes located along the leading edge of five vanes and two struts. Static pressure taps were installed in the hub and shroud. In the core flowpath, total pressure and temperature probes were installed along the leading edge of the IGV's, EGV1, and the core strut. Static pressure taps were located on the hub and shroud which were used as indicators of ice. Metal thermocouples embedded

below the surface were also installed along the booster and outer shroud in the same locations as the previous test<sup>3</sup> (Fig. 5) since this had been the primary method to detect icing during that test. The icing that results in the rollback events for this engine configuration has been thought to occur in the single-stage booster section. During the test, four internal engine cameras were installed in different circumferential positions around the booster section, shown in Fig. 5. Three cameras focused on the EGV2 trailing edges and one camera aimed downstream of the EGVs near the shroud. In each camera view the NASA icing sensors could be seen. This enabled the data from the sensors to be correlated to the camera views for instrumentation validation and development. Additional details of the engine instrumentation can be found in Goodwin et al.<sup>14</sup>

NASA has a strong interest to understand the effects the engine fan has on the icing cloud. In an effort to begin characterizing the cloud aft of the fan, light extinction probes (LEP) were used. Laser tomography was used to monitor cloud uniformity upstream of the fan, this is also used during the cloud calibrations.<sup>15</sup> The light extinction probes look at the cloud in four planes: behind the fan, bypass duct inlet, core inlet, and bypass duct exit. The locations of these probes are shown in Fig. 4. The LEP's work on the principle of light extinction in that a laser beam is projected to a sensor through the cloud particles. The sensor measures how much energy was able to pass through the cloud. The theory is that by correlating the cloud measurements upstream and aft of the fan, the effect of the fan on the cloud ingested into the core flow path can be investigated.

Humidity or water vapor content measurements were made of samples continuously pulled from upstream and downstream of the HPC. Analysis of this data could reveal how much of the total water content of the cloud was actually moving into the core flow path aft of the fan. The water vapor content of the air is also related to the icing potential from evaporative cooling in the LPC which could be a key factor in understanding the physics of ice crystal icing.

Advanced techniques to detect ice were explored through a series of ice detection sensors. The capacitance based icing sensors developed at NASA were installed in the outer shroud region near the EGV2 trailing edge and were captured by all of the cameras looking at the inner flow path. The objective was to detect clean or contaminated surfaces during cloud on testing and to distinguish liquid water from solid ice contaminations. Through a NASA Memorandum of Understanding, National Research Council of Canada (NRC) participated in this test to evaluate their ice detection sensor technology.<sup>14</sup> NRC developed an ultrasonic sensor and a number of them were mounted external to the flow path. The NRC external sensors were installed in regions close to the NASA sensors to investigate if the readings made by both sensors corroborated well with camera images and with each other. Along with the sensors, NRC also provided a system that measures humidity under mixed-phase conditions.<sup>14,17</sup>

A Raman Scattering Surface Water probe was installed in the s-duct upstream of the HPC to evaluate how effective the technique of Raman scattering could detect the presence and temperature of water/ice flowing past the probe.

Dynamic pressure sensors (Kulites) were installed in all stages of the HPC in order to investigate the pressure changes within the stages of the HPC during the ingestion of ice that shed upstream of the HPC.

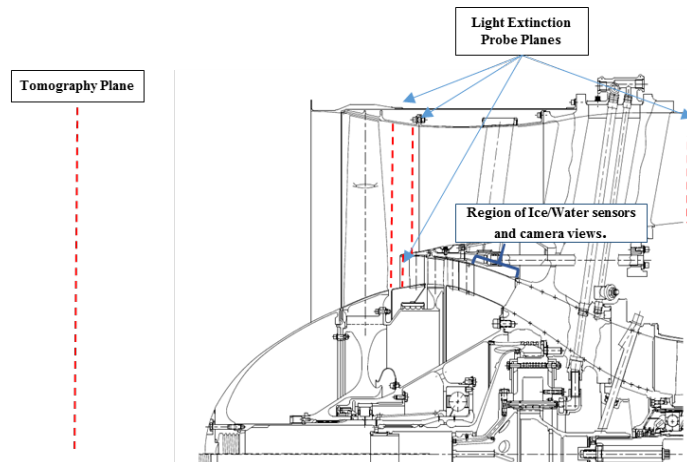


**Figure 4. Advanced Instrumentation Locations in an Unmodified ALF502R-5 Engine Fan and Booster Section.<sup>3</sup>**

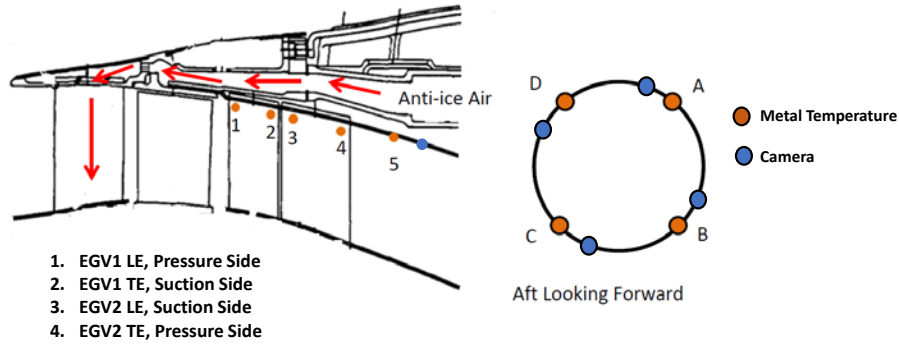


Figure 5. Metal Temperature and Camera Locations.

## VI. Experimental Results

As Discussed in Goodwin et al.<sup>3</sup>, this unmodified engine model experienced several in-flight rollback events over a narrow window of ambient temperature and altitude conditions shown in Fig. 6. The colored dots represent the revenue service points replicated during the PSL LF01 and LF11 tests. The FLT850 and FLT855 points were key points from the Honeywell 1997 flight test with the LF01 engine and were repeated during the PSL LF01 and LF11 tests. During the flight test, the engine operating parameters, aircraft flight altitude, and instrumentation response were documented. The PSL facility was set-up to replicate the atmospheric and initial engine operating conditions from the flight tests. The 1997 flight test had a high level of uncertainty in the *TWC* measurement on the order of  $-0.5 \text{ g/m}^3$  and  $+1.0 \text{ g/m}^3$  from the original measurement made using a hotwire probe.<sup>17,18</sup> During both PSL tests, the data show the engine will rollback over a large range of *TWC*, based on multi-wire measurements, at the FLT850 condition. As the *TWC* increases, the time to rollback the engine decreases. During the PSL LF01 test, three *TWC* values were run to full rollback at the FLT850 condition.<sup>2</sup> The lowest *TWC* full rollback case matched the engine response time experienced during the flight test. Further analysis of the results revealed that the thermocouple behavior from the PSL test was very similar to the flight test response.<sup>2</sup> Measurement uncertainties from the flight test also existed with the cloud *MVD*. Data discussed later will show that this uncertainty has a very limited effect on the rollback response.

To replicate the revenue service points, since they were not tested during the Honeywell flight test, the customer deck from Honeywell determined the engine operation at the known ambient temperature, pressure, and altitude from the event data.

The following results will show initial data that explores the facility capability and identifies key conditions that affect the engine response. The data will also look at the accretion due to altitude effects.

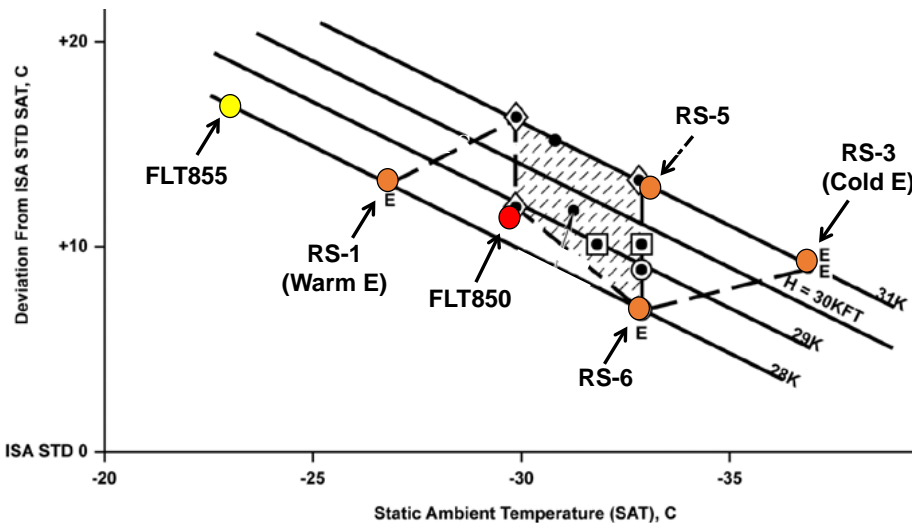


Figure 6. Altitude and Temperature Window of Field Events Repeated in LF11 Test.

### A. Repeatability of Similar Engines

Full engine rollback as experienced during the 1997 flight test (FLT850)<sup>3</sup> was replicated during the LF01 test<sup>2</sup>. In this current study with the LF11 engine, the FLT850 point was simulated with several different TWC values. A full rollback was conducted at the “fast” rollback TWC value from the LF01 PSL test. A comparison of the LF01 and LF11 fast rollback point for FLT850 condition is shown in Fig. 7. The dashed line represents the LF01 engine response and the solid line is the heavily instrumented LF11 engine response. The engine responses (load, fan speed, average booster temperatures) between both engines show good repeatability. Although the initial load (red line) is higher for the PSL LF01 test, the rate of load reduction is similar for both tests. Likewise, *N1*, *N2*, and the booster temperature behaved in a very similar manner between the two tests. It was found that the load began to decrease roughly three seconds prior to *N1* reduction. The LF11 engine had a faster initial response when the cloud was turned on which can be attributed to the initial larger blockage due to the leading edge aero instrumentation. Once the cloud is turned on, the load and *N1* responds rapidly until they reach a point (see arrow in Fig. 7) where the reduction is steady. It is at this point where the two engine measurements nearly overlap. The LF01 engine does reach a full rollback just before the LF11 engine. Prior the engine test in PSL, Honeywell conducted a baseline performance test at their facility. These tests revealed slight performance differences between the two engines which could also contribute to the minor discrepancies.<sup>19</sup>

To understand how well PSL can replicate similar engine responses for the same engine model, ten key revenue service and research points from the PSL LF01 engine test were repeated in the current study. These points, not all rollback conditions, were all run in a called rollback mode. A comparison of the load, fan speed, compressor speed, and average metal temperatures along the flowpath are shown for five conditions in Fig. 8. The figures focus on the time the cloud was on for the LF11 test. In some cases the PSL LF01 cloud spray was longer. The load, fan speed, and compressor speed show good repeatability over the different conditions, including altitude changes (Fig. 8d and Fig. 8e). It is noted that there is a faster load response in Fig. 8b for the Warm E condition. It was found during the test that this condition was very sensitive to rollback (i.e. threshold) and slight variations of parameters could turn on or off rollback and alter rollback time. Further investigation reveals that the station 1 static temperature was 1.48°F lower during the LF11 test which could have an effect on the rollback time. Once the cloud is on, Fig. 8b shows that the average metal temperatures for LF11 are reading much colder, indicating that some ice buildup is occurring sooner and corresponds to the faster load reduction. For each test condition the metal temperatures are consistently slightly lower for the PSL LF11 test. It is evident that there is a correlation between the metal temperature and load/fan response. The 35kft altitude research point also shows a load response variation from each test. It is unclear what caused the load increase during the LF01 spray in Fig. 8e. The data indicates that there is no adjustment to the PLA setting and there isn't a sharp temperature fluctuation which could reveal an ice buildup or shed ice event which could impact the load response. Prior to this spike in load, the LF01 and LF11 results were very repeatable. The load spike in LF01 re-set the response which led to a slower call rollback. Further investigation is needed to understand the fluctuation observed in the PSL LF01 data.

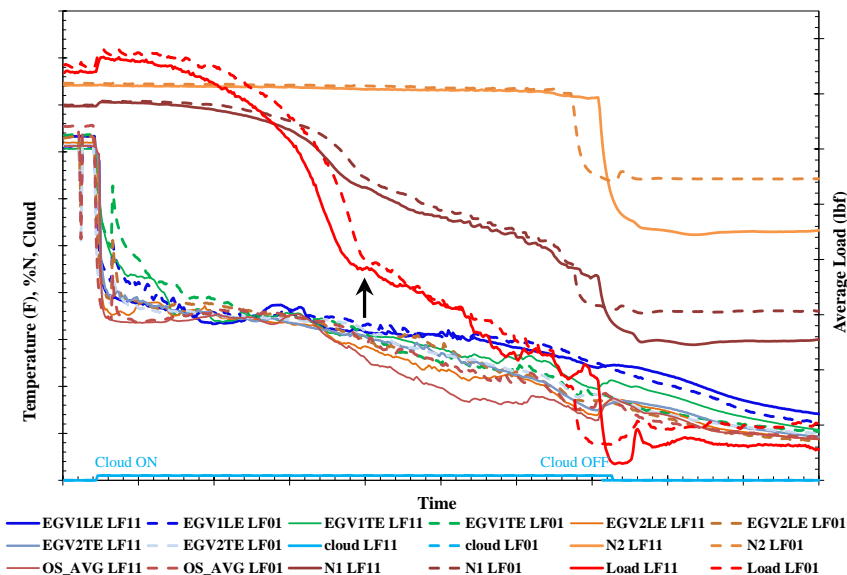
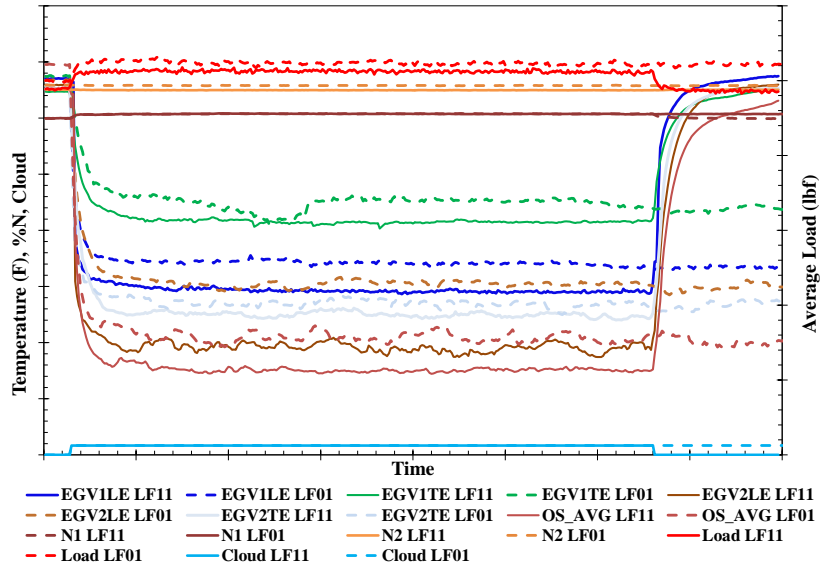


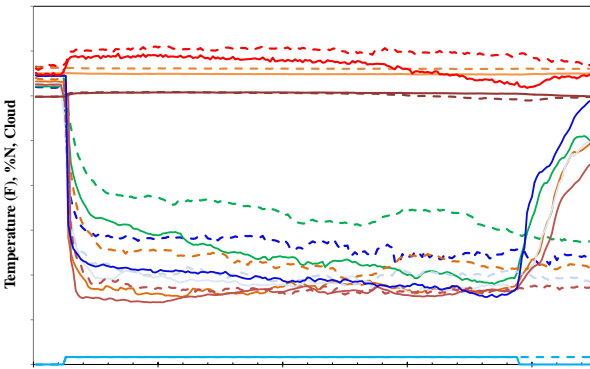
Figure 7. LF01 (dashed) and LF11 (solid) FLT850 Full Rollback Points

FLT855



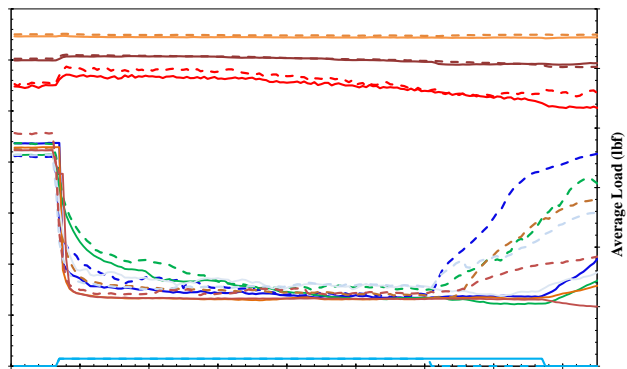
(a)

Warm E



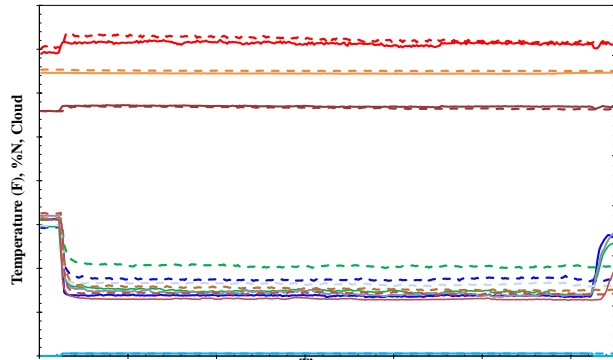
(b)

Cold E



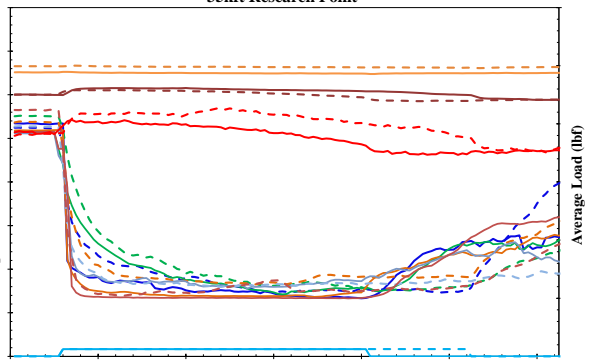
(c)

5kft Research Point



(d)

35kft Research Point



(e)

Figure 8. Comparison of PSL LF11 and LF01 Engine Response.

## B. Daily Engine Repeatability

In order to ensure the engine and facility are operating properly and consistently producing the correct conditions, the first spray of almost every test day was a FLT850 anchor point. This point was at the FLT850 operating conditions and at a specific cloud setting. Figure 9 shows all of the anchor points run during the test entry with the same engine configuration. During two test days the engine was run with an insulated spinner (i.e. no spinner heat). For consistency, those anchor points are not shown in Fig. 9. It is important to note that when they are plotted out with the other anchor points, the insulated spinner anchor points fall right on top of the data.

Fan speed, EGV1 trailing edge average metal temperatures, and the normalized load is show in Figs.9a-9c. The day-to-day repeatability of the engine response is very good. The standard deviation of the fan speed is 0.22%, temperature is 3.07°F, and load is 15.48 lbf for the cloud on time period. Performance degradation due to blade damage and/or buildup of mineral deposits on the blade surfaces from using filtered city water was observed throughout the test. In Fig. 9a and Fig. 9c there is a small data shift for readings 178 (gray line) and 179 (yellow line). Prior to the Rdg 178/179 test day the engine experienced a flameout and that afternoon an engine wash was performed on the engine. Although a performance shift was not observed, it is speculated that engine damage may have occurred which was discovered after the following run.

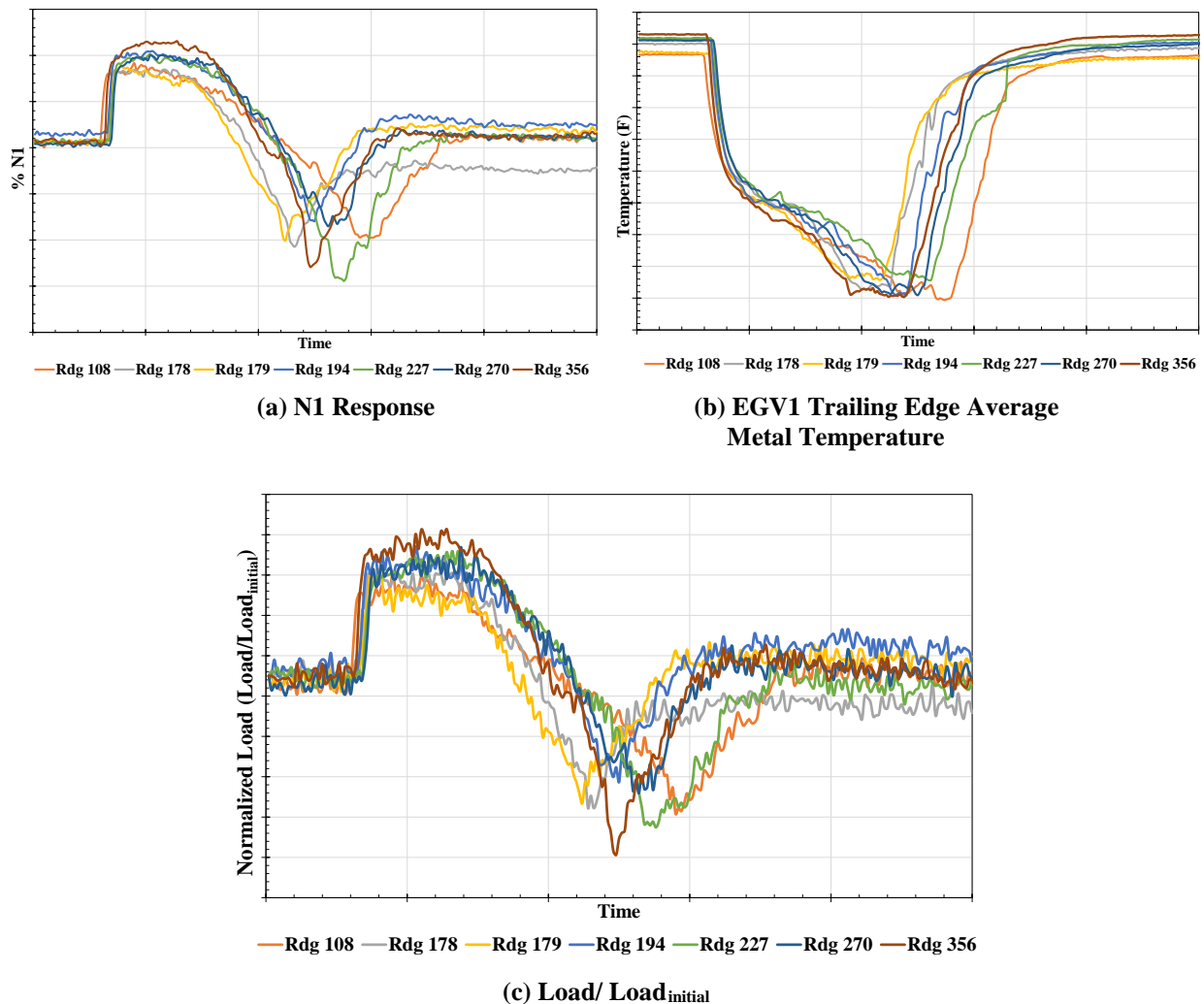


Figure 9 Fan Speed Response (a), EGV1 Trailing Edge Average Metal Temperature (b), and Normalized Load (c) for all FLT850 Anchor Points.

### C. Effects of Icing

The purpose of this work is to understand how ice crystal icing impacts engine performance. Due to the direct connect nature of the facility, once the cloud is turned on both the facility and engine are affected. This section will explore how ice crystal icing affects the engine response and facility.

**Metal Temperature Response**—Metal temperatures were obtained at five axial locations in the booster section, see Fig. 5. The metal temperature behavior in the booster flowpath are tracked at every other scan during a FLT850 anchor point in Fig. 10. Prior to the cloud turning on, the temperatures in the flowpath are nearly uniform. The metal temperatures begin to decrease once the cloud turns on and sharply decreases two seconds after the cloud starts. The ice crystal cloud impinges on the EGV leading edges cooling the metal temperatures. The video data shows immediate runback on the outer shroud, see Fig. 11, from the liquid water/ ice mixed-phase cloud particles being centrifuged outwards and then impacting the outer wall which cools the surface. This is also evident in the outer shroud metal temperature in Fig. 10. As the spray continues, the metal temperatures continue to decrease as the ice accretes. Once the trailing edges of the exit guide vanes reach the same temperature as the leading edge temperature, the load steadily decreased and for this case there was a called rollback. This temperature behavior was observed for the called rollback cases analyzed. Although significant ice accretion could be observed on the outer shroud region, it is important to note that the blockage that is the main cause of rollback could not be fully observed at the camera angles and had to rely on the thermocouple measurements.

Although ice and/or water may be present for any given particular condition, it was found that it didn't always lead to a rollback. During a FLT850 condition the  $N1$  was increased by 5% which led to a non-rollback. The still image from this condition is shown in Fig. 12 and traces of water and ice can be seen on the outer shroud region. The average metal temperatures for this case is plotted in Fig. 13. The axial temperature fluctuation is similar for the called rollback case in Fig.10. However, the temperatures do not rapidly decrease when the cloud is turned on and reach similar temperatures. This suggests that the added heat from the increased  $N1$  promotes little accretion and no rollback.

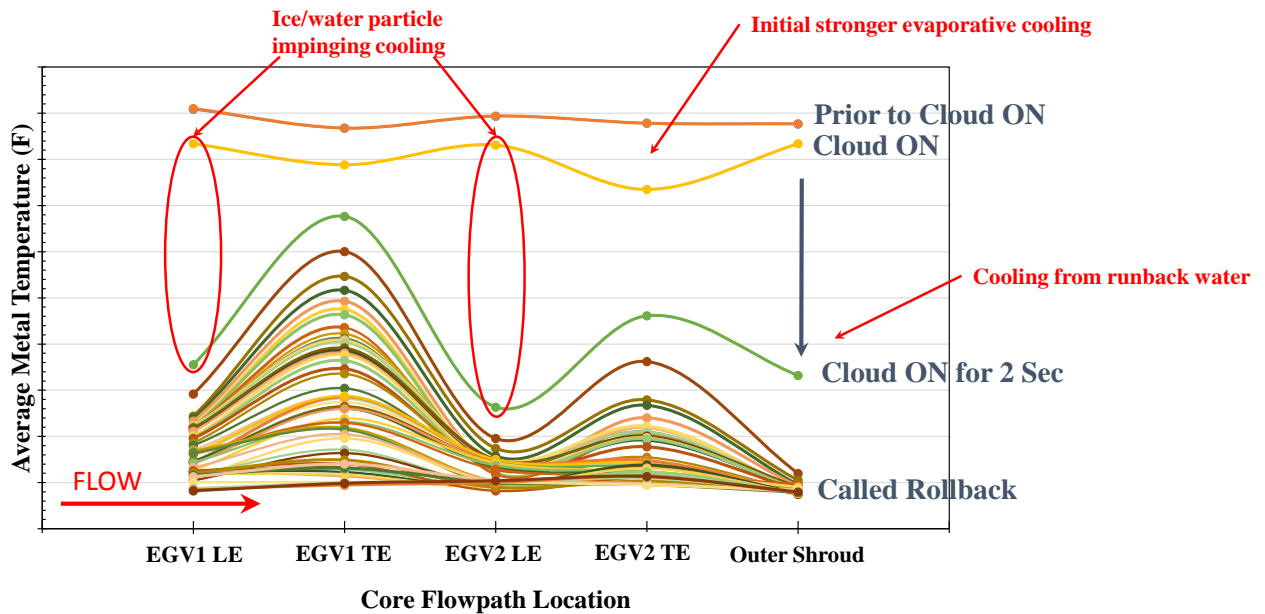


Figure 10. Time Trace of Average Metal Temperatures in Booster Section for FLT850 Called Rollback.



Figure 11. Runback example.



Figure 12. Example of Accretion for FLT850 Non-Rollback.

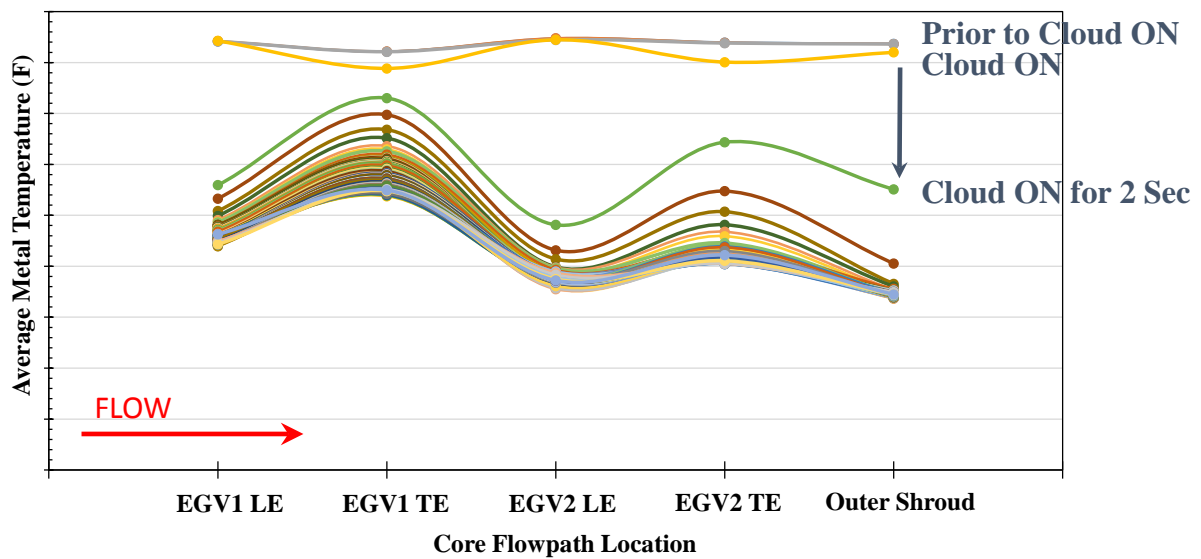
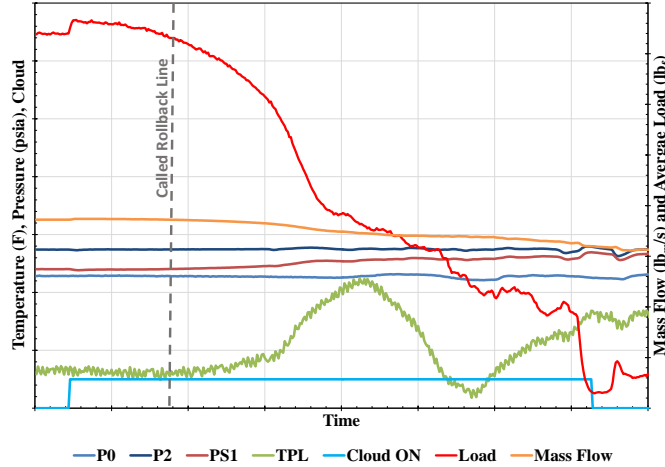


Figure 13. Time Trace of Average Metal Temperatures in Booster Section for FLT850 Non-Rollback.

**Facility Response Due to Rollback**—The PSL facility is a direct connect facility and can be influenced by the engine response during an icing event. When the ice begins to accrete, the load and N1 begins to reduce, as seen in Fig. 14 and Fig. 7. The facility conditions are set by  $P_0$ ,  $P_2$ , and the plenum temperature. Figure 14 shows that those conditions hold very steady throughout the test. As the load reduces the plenum temperature (TPL) spikes and tries to recover at the second load reduction point. It is also noted that far into the spray, the air mass flow rate begins to reduce. Only one full rollback point was run and all the other test points were run to a CRB, for engine safety. The notional CRB point for this FLT850 condition is shown as a dashed line in Fig. 14a. It is noted that the facility conditions and mass flow remain very steady over this time period from cloud on to CRB. This was evident in other CRB test cases analyzed.



**Facility Conditions and Compressor Inlet Static Pressure**  
**Figure 14. Pressure and Temperature Response During Full Rollback.**

**Accretion and Shedding**—The un-modified ALF502R-5 engine was primarily susceptible to ice accretion from ice crystal ingestion causing rollback to occur. During several research points, ice buildup and immediate ice shedding was observed. Possible ice buildup and shedding was also observed from the metal thermocouple response in LF01. The LF11 thermocouples, which measured the outer shroud temperatures are shown in Fig. 15, were correlated to the videos. When the cloud is turned on, evaporative cooling on the metal surfaces causes the temperatures to decrease rapidly. As ice builds, the temperatures continue to decrease. In the case of the test point in Fig. 15, there was not enough accretion to cause an additional temperature decrease and subsequent rollback as observed in Fig. 10. However there are temperature spikes that correlate to the ice building and shedding on the outer shroud surface.

There was one instance, during an engine recovery (i.e. cloud off), a large ice shed event occurred which resulted in an unexpected engine flameout. It was speculated that this caused some initial engine damage. Future investigation is needed to see if the instrumentation used in this study can track the large shed ice through the engine.

### Outer Shroud Metal Temperatures Aft of EGV2

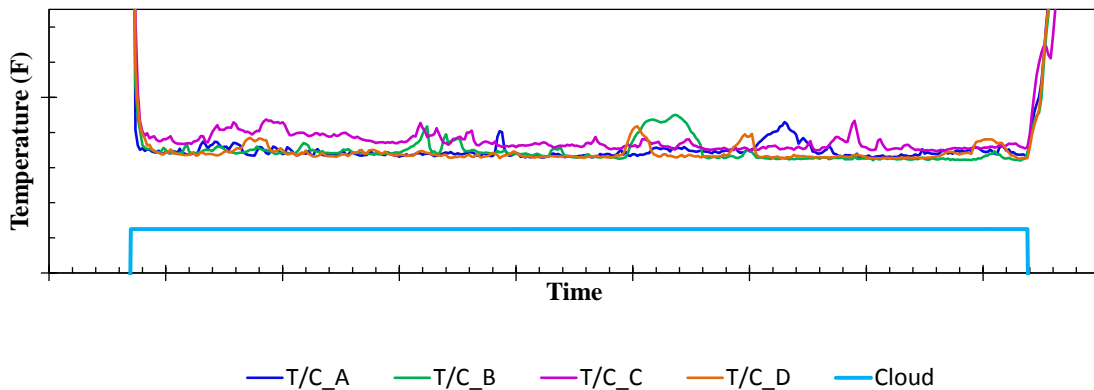


**Figure 15. Outer Shroud Metal Temperatures.**

#### D. Influences on Rollback

Data were acquired at key revenue service and research points. To understand the influences of ice accretion, independent sweeps of *MVD*, *TWC*, fan speed, and ambient temperature were performed. Other more local icing

condition focused parameters were explored to assess their effects. These efforts are discussed in Dischinger et al.<sup>20</sup> This engine featured a heated spinner and IGV anti-ice system. A study was conducted to understand the effects of those heat sources. The following will describe some of the preliminary findings from those studies as well, focusing mainly on the steady state data and the internal cameras.

**TWC Effects**—Total water content played a crucial role to the onset and rate of ice accretion. The *TWC* values in this sections from a bulk calculation based on the ratio of the water injection to air mass flow rate around a 24” diameter.<sup>12</sup> This calculation is very similar to the bulk measurements acquired with the Iso-Kinetic probe (IKP). This bulk calculation extrapolates the center value from the IKP measurement based on the intensity from inlet tomography measurement during the cloud calibration.<sup>12</sup> It was found that the IKP measures a higher *TWC* as compared to the multi-wire probe<sup>13</sup> by a factor of about 2 for ice crystal conditions only. This is comparable to the measurement assessment made on the instrumentation used during Honeywell’s flight test.<sup>18</sup> The effect of *TWC* on the load and *NI* response can be seen in Fig. 16 for the FLT850 condition. The markers for the cloud indicate when there was a CRB and the cloud was turned off. Sixty second sweeps were performed for each point. However only *TWC*’s of 3.3 g/m<sup>3</sup> (Rdg 122) and greater resulted in called rollbacks within the sweep period. In Fig. 16, the fan speed and load response had little effects at the lower *TWC*. Once the *TWC* exceeded 2.3 g/m<sup>3</sup> there was more ice buildup in the core flowpath, resulting in accelerated load and fan speed reduction. It was observed that for many of the research points explored, increasing the *TWC* could force a rollback.

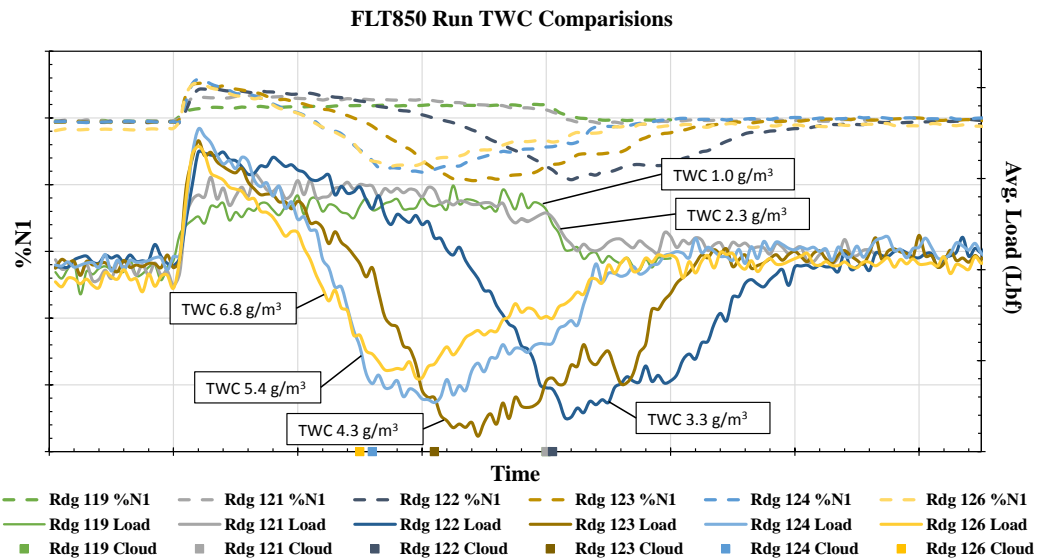
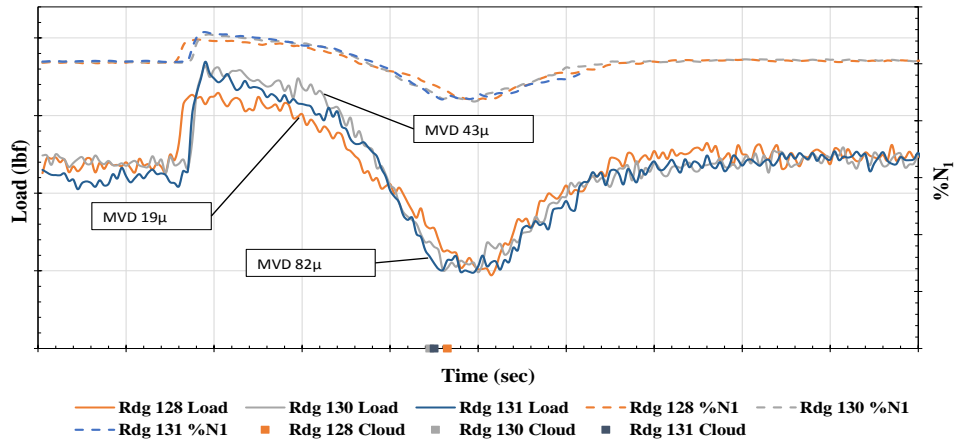


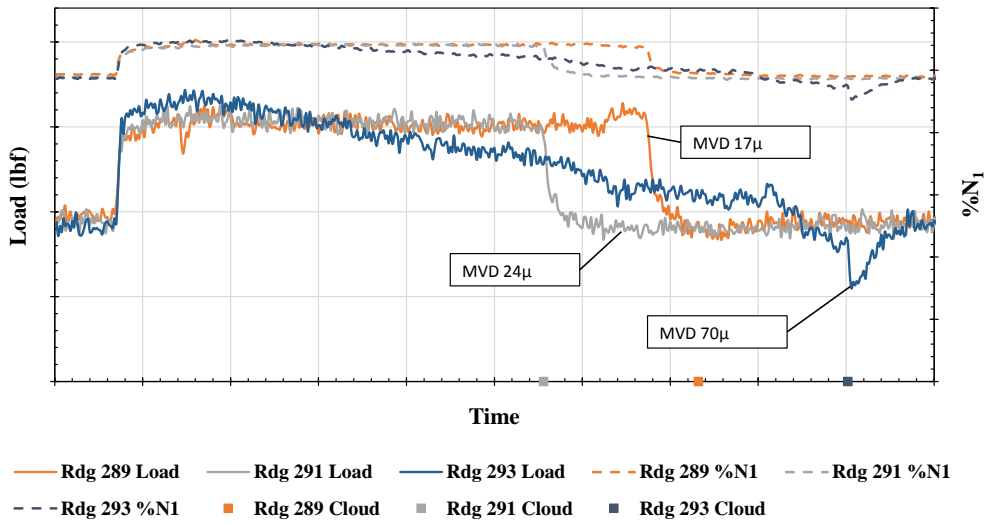
**Figure 16. Effect of TWC on Load and Fan Speed at FLT850 condition.**

**MVD Effects**—The influence of ice particle size was studied through a series of *MVD* sweeps for several key revenue and research points. It was found that for conditions in regions of strong ice buildup, such as the FLT 850 condition, *MVD* has little effect. This is observed in Fig. 17a. Both the load and fan speed response has little effect from the three *MVD* sizes. In contrast, for conditions in threshold regions of slow ice buildup such as the Warm E (Fig 17b) and Cold E (Fig. 17c) conditions, the *MVD* has an enhancing effect on the rate of ice buildup in the EGV region. In Fig. 17b, the particle sizes have no effect for an *MVD* of 17µm and 24µm and the condition does not rollback. However once the particle size increases to 70µm, accretion occurs that leads to a called rollback. In Fig. 17c increasing the *MVD* enhances the icing which decreases the CRB time, as seen by the engine response and the cloud off markers.

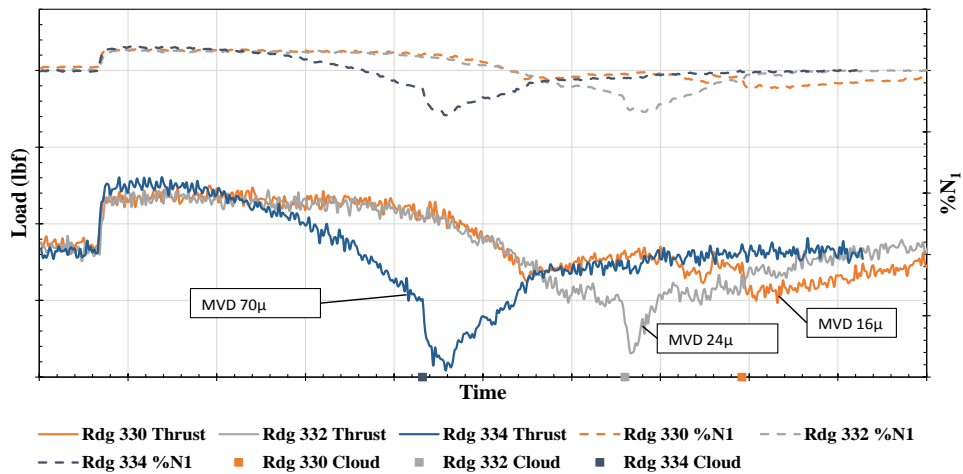
Understanding the potential influence of *MVD* is of importance as the current PSL capability cannot replicate the estimated particle size distributions and morphological features that are being suggested from from high ice-water content flight tests. Successful replication of the rollback events in both PSL LF01 and LF11 tests indicate that the ice particles are much smaller once they pass through the fan and enter the core flowpath. Analysis with the COMDES code suggests that particle sizes that are being entrained in the core flowpath are on the order of 5 microns.<sup>5</sup> This current study used Light Extinction Probes that were able to measure the ice particle bulk concentration just aft of the fan and at the inlet of the bypass and core.



(a) FLT 850



(b) Warm E



(c) Cold E

Figure 17. MVD Comparisons for (a) FLT 850 (b) Warm E and (c) Cold E Conditions.

**Fan Speed (*N1*) Effects**—*N1* sweeps were performed for several revenue service and research conditions. Figure 18 shows a large sweep that was performed over the FLT850 condition. It was found that increasing *N1* can be an effective way to increase the temperature in the core flowpath and suppress accretion, which was also observed in Fig. 13. This method was used to explore modeling points (altitude and research points) for the 1D COMDES code assessment.<sup>4</sup> Once the fan speed was increased slightly above the cruise operating point (*N1*), the EGV1 average metal temperatures remain significantly higher due to added energy in the flow, see Fig. 19. These increased *N1* conditions were both non-rollbacks. However, the video data show that there was still some slushy ice building and shedding in the outer shroud region. Decreasing *N1*, which decreases the initial metal temperatures, shows stronger evaporative cooling is occurring in the boosters leading to a faster accretion and rollback. It was noted that little to no water runback was observed for these lower *N1* conditions. This behavior is consistent with what was observed during the ambient temperature sweeps.

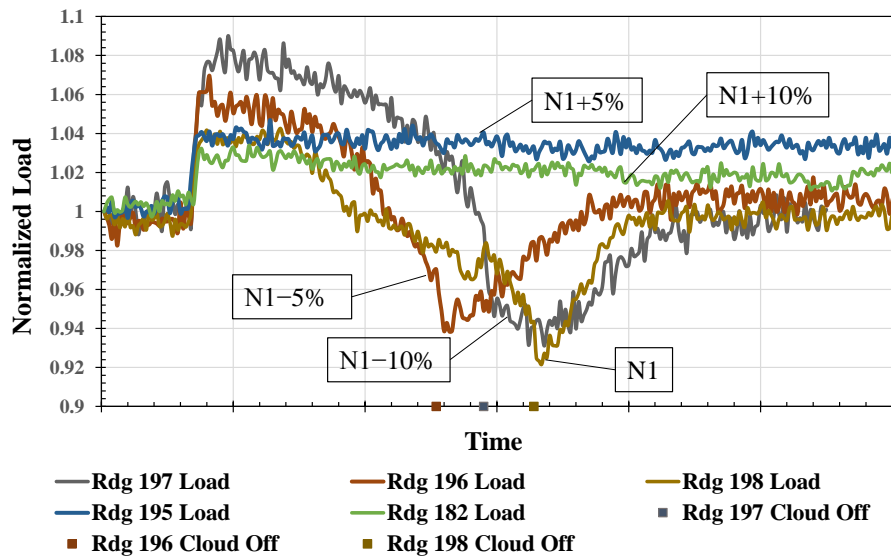


Figure 18. Effect of *N1* on the Normalized Load for FLT850.

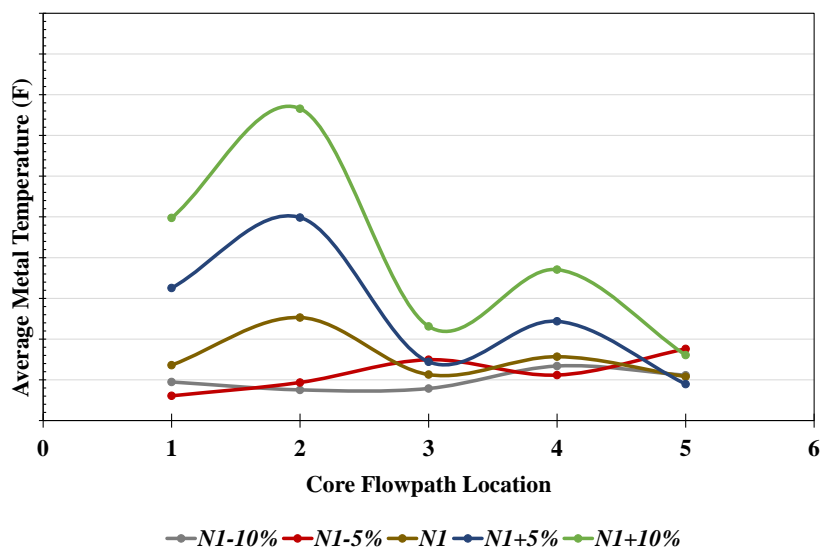
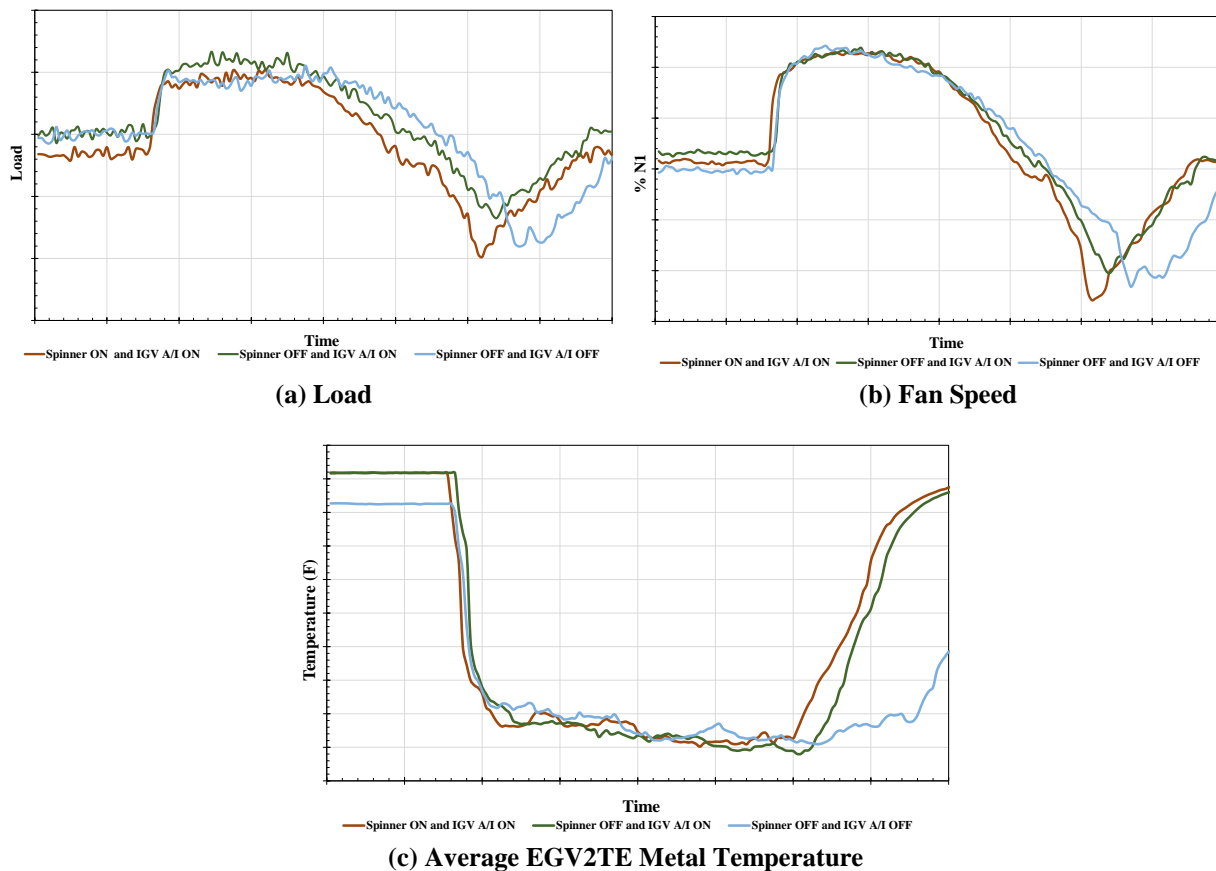


Figure 19. Average Metal Temperature at Final Cloud ON Reading.

**Effect of Heat Sources**—For this particular engine model, there are three potential sources of liquid water: in situ heating of the ice particles in the air and upon impact, the heated spinner, and the IGV anti-ice heat. In Fig. 20, the load (a), fan speed (b), and EGV2 trailing edge average metal temperatures (c) are shown for three different heat source configurations at the FLT850 test condition. The spinner and IGV anti-ice are heat sources that potentially can produce liquid water which promotes rollback. When all three sources are present, this creates more liquid water available in the flowpath which promotes faster ice buildup and leading to a quicker rollback. When the spinner heat is turned off and the IGV anti-ice and in situ heating are present, the ice formation is slightly slower which leads to a medium speed rollback. When there is in situ heating only, there is a slower rollback due to the less amount of runback liquid water on the core flowpath surfaces. It is interesting to note that when the IGV anti-ice heat is turned off the liquid water is attributed to in situ heating and spinner heat. This causes the accretion to be very slow yet eventually leads to a rollback. This is not shown in Fig. 20 for consistency because it was run for a slightly different operating point. In the previous LF01 PSL test, the anti-ice off configuration was only run for a short period of time which did not allow the accretion development. During the LF11 test, the icing spray times were extended to see the full influence of the heat sources. It was found that rollback is imminent regardless of whether the heat sources are present or not for the FLT850 condition.

For this study little to no ice accretion was seen on the lower 1/3 (i.e. near the hub) of the IGV's, even when the anti-ice was turned off. A visible liquid water layer was not observed during this study as in the LF01 test.



**Figure 20. Engine Configuration Effects on (a) Load, (b) Fan Speed, and (c) EGV2 Trailing Edge Metal Temperature.**

**Effect of Altitude**—Research data were acquired outside of the LF11 engine operating range to study altitude effects. The NASA COMDES code was used to find operating conditions at 5k ft. that could result in a rollback. A series of *TWC* and ambient temperature sweeps were conducted. For a given *TWC* the COMDES model found several fan speed and ambient temperature combinations which could lead to a potential called rollback. Figure 21(a) shows very heavy ice accretion along the outer shroud at the 5K ft. called rollback point. This is compared to the called rollback point associated with the FLT850 fast rollback as shown in Figure 17(b). This altitude dataset will help compliment previous efforts to evaluate possible altitude scaling methods for simulating engine ice crystal icing in PSL.<sup>22, 23</sup>



**Figure 21. Ice Accretion at (a) 5 Kft Research Point and (b) FLT850 at Respective CRB Times.**

### E. Other Observations

To further explore the capability of the facility, a descent operation point was exercised. For this operation the engine and facility were set to the FLT850 anchor point condition. Once the spray turned on, the facility remained at the FLT850 point until the engine reached a called rollback. The cloud was then turned off and the engine was taken down to flight idle. Once at flight idle, the facility simulated a descent profile, by controlling the pressures and temperature, to approximately 14kft. This test point is shown in Fig. 22.

Another test point of interest to the research community is the influence of peak intensity which could be experienced by the aircraft flying through regions of peak *TWC*. The condition selection process is described in Dischinger et al.<sup>20</sup> Three peak *TWC* configurations were run, each with varying time in the peak *TWC* condition. The facility spray bars were pre-programmed for easy transition between the low and high *TWCs*. Future work may include investigation of these points.

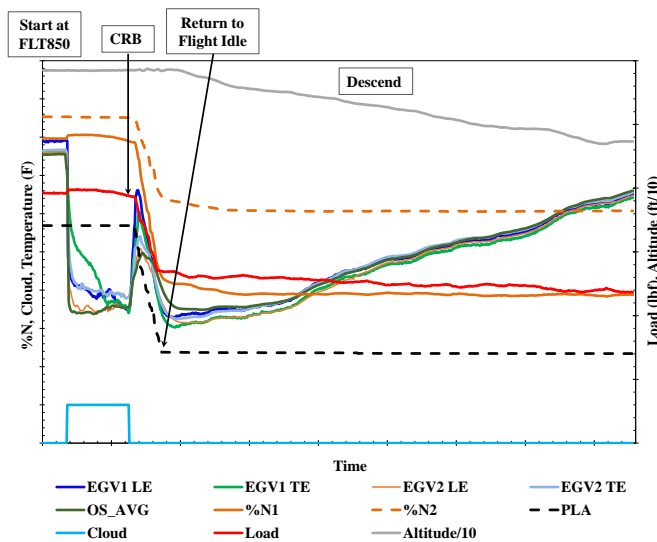


**Figure 22. Engine and Facility Response During Descent Operation.**

## VII. Conclusions

A heavily instrumented, unmodified ALF502R-5 engine was installed in the PSL facility and repeated the FLT850 full rollback point with very good agreement to the LF01 full rollback. Several key revenue service points and altitude research points were repeated from the previous LF01 PSL test. The data show good agreement between the engine response from the LF01 and LF11 engines despite the fact that the LF11 engine was heavily instrumented. A specific FLT850 condition (anchor point) was run at the beginning of nearly every test day to evaluate the repeatability of the engine behavior and PSL facility. The data show that although there was a slight performance degradation throughout the test due to the contamination of city water, the engine and conditions were very repeatable.

The video acquired for each test point reveal that when the cloud is turned on for CRB cases, there is immediate water runback indicating a mixed-phase condition in the booster (LPC). The ice accretion was observed on the outer shroud region of the exit guide vanes. The blockage that is the main cause of rollback could not be fully observed at the camera angles. Tracking the metal thermocouple response through the booster show the leading edges of the EGVs are cooled due to ice/water impingement. The data show the outer shroud metal temperatures decrease rapidly due to the strong evaporative cooling from the water runback due to the centrifuging effects. As the ice accretes on the outer shroud, the thermocouples measurements indicate possible ice building in the EGV2 region and moving forward causing the trailing edge thermocouples to reach near freezing levels like the leading edge and outer shroud regions. In some cases, the thermocouples picked up ice buildup and sheds which correlated to the observations made in the video.

For each condition selected, additional sweeps of the *TWC*, *MVD*, *NI*, and ambient temperature were conducted. The data show that for this engine, the *TWC* can have the largest effect on the onset of icing whereas *MVD* is a secondary effect. For strong accretion conditions, *MVD* had little to no effect. For threshold conditions, especially in colder threshold regions, increasing the *MVD* has similar effects as increasing *TWC* where the additional water increases the rate of accretion and decreases rollback time. The *NI* sweep data show that decreasing the fan speed promotes stronger cooling leading to an increased rate of accretion. Increasing the fan speed raises the EGV1 temperatures and the accretion does not result in a rollback. This behavior is consistent with what was observed during the temperature sweeps.

The data show that the additional heat sources from the spinner heat and IGV anti-ice system promote accretion and rollback. However, those sources are not needed for rollback to occur. When additional heat sources are removed, the engine has a slower rollback time.

Additional conditions were explored, though not fully described in this paper. The PSL facility demonstrated the ability to simulate peak *TWC* intensities during a single spray and performed a flight descent. In addition to performing various parametric sweeps for a specific flight condition, a series of runs were performed that isolate particular engine effects.

The data generated during this test is being used to validate the in-house icing prediction and risk mitigation computational tools. The data also enables the assessment and development of the advanced instrumentation and expands the capabilities of the Propulsion Systems Laboratory by generating test methodologies.

## Acknowledgements

This work was supported under the NASA Advanced Air Vehicles Program, Advanced Air Transport Technology Project and the Aeronautics and Evaluation Test Capability Project. The authors would like to acknowledge Dr. Judith Van Zante for providing icing cloud expertise, Tim Bencic for developing and acquiring the advanced instrumentation measurements, Joe Veres and Phil Jorgenson for providing COMDES results, Paul Tsao for technical guidance, and the rest of the Engine icing team for their expertise. The authors would like to thank the entire PSL staff for their dedication and support of this test. The authors also wish to thank Ron Goodwin, Bob Ciero, Dave Dischinger, Paul Gustafson, Terry Neal, Dan Walker, and the rest of the Honeywell team for their contributions during the engine test under the NASA collaborative Research and Technologies for Aerospace Propulsion Systems (RTAPS) contract effort. The authors would also like to acknowledge the Ice Crystal Consortium whom provided support to Honeywell.

## References

- <sup>1</sup>Griffin, T.A., Lizanich, P., and Dicki, D.J., "PSL Icing Facility Upgrade Overview," *6th AIAA Atmospheric and Space Environments Conference*, Atlanta, GA, June 16-20, 2014, AIAA 2014-2896.
- <sup>2</sup>Oliver, M. J. "Validation Ice Crystal Icing Engine Test in the Propulsion Systems Laboratory at NASA Glenn Research Center," *6th AIAA Atmospheric and Space Environments Conference*, Atlanta, GA, June 16-20, 2014, AIAA-2014-2898.
- <sup>3</sup>Goodwin, R.V., Dischinger, D.G., "Turbofan Ice Crystal Rollback Investigation and Preparations Leading to Inaugural Ice Crystal Engine Test at NASA PSL-3 Facility," *6th AIAA Atmospheric and Space Environments Conference*, Atlanta, GA, June 16-20, 2014, AIAA-2014-2895.
- <sup>4</sup>Veres, J.P., Jorgenson P. C. E., Jones, S. M., "Modeling of Highly Instrumented Honeywell Turbofan Engine Tested with Ice Crystal Ingestion in the NASA Propulsion System Laboratory," submitted to 2016 AIAA Aviation. *8th AIAA Atmospheric and Space Environments Conference*, Washington, D.C, June 13-17, 2016.
- <sup>5</sup>Veres, J.P., Jones, S.M., Jorgenson, P.C.E., "Performance Modeling of Honeywell Turbofan Engine Tested with Ice Crystal Ingestion in the NASA Propulsion System Laboratory," *SAE 2015 International Conference on Aircraft and Engine Icing and Ground Deicing*, 2015-01-2133.
- <sup>6</sup>Jorgenson, P. C. E., Veres, J. P., Coennen, R., "Modeling of Commercial Turbofan Engine with Ice Crystal Ingestion; Follow-On," *6th AIAA Atmospheric and Space Environments Conference*, Atlanta, GA, June 16-20, 2014, AIAA-2014-2899 and NASA/TM-2014-218496.
- <sup>7</sup>Veres, J. P., Jorgenson, P. C. E., "Modeling Commercial Turbofan Engine Icing Risk with Ice Crystal Ingestion," *5th AIAA Atmospheric and Space Environments Conference*, San Diego, CA, June 24-27, 2013, AIAA 2013-2679 and NASA/TM-2013-218097.
- <sup>8</sup>Struk, P.M., Bencic, T.M., Tsao, J., B., Fuleki, D., Knezevici, D. C., "Preparation for Scaling Studies of Ice-Crystal Icing at the NRC Research Altitude Test Facility," *5th AIAA Atmospheric and Space Environment Conference*, San Diego, CA, June 24-27, 2013, AIAA-2013-2675, also NASA/TM-2013-216571.
- <sup>9</sup>Struk, P., Currie, T., Wright, W. B., Knezevici, D. C., Fuleki, D., Broeren, A., Vargas, M., and Tsao, J. "Fundamental Ice Crystal Accretion Physics Studies," *SAE 2011 International Conference on Aircraft and Engine Icing and Ground Deicing*, 2011-38-0018 or NASA/TM—2012-217429, 2012.
- <sup>10</sup>Currie, T. C., Struk, P. M., Tsao, J., Fuleki, D., and Knezevici, D. C. "Fundamental Study of Mixed-Phase Icing with Application to Ice Crystal Accretion in Aircraft Jet Engines," *4th Atmospheric and Space Environments Conference*, AIAA 2012-3035, 2012.
- <sup>11</sup>Soeder, Ronald H., Sheldon, David W., Ide, Robert F., Spera, David A., and Andracchio, Charles R., "NASA Glenn Icing Research Tunnel User Manual," NASA/TM—2003-212004, 2003.
- <sup>12</sup>Van Zante, J.F., Bencic, T.J., and Ratvasky, T.P., "Update on the NASA Glenn Propulsion Systems Lab Ice Crystal Cloud Characterization (2015)," submitted to 2016 AIAA Aviation. *8th AIAA Atmospheric and Space Environments Conference*, Washington, D.C, June 13-17, 2016, AIAA 2016-xxxx.
- <sup>13</sup>Van Zante, J. F., and Rosine, B. M. "NASA Glenn Propulsion Systems Lab: 2012 Inaugural Ice Crystal Cloud Calibration," *6th AIAA Atmospheric and Space Environments Conference*, Atlanta, GA, June 16-20, 2014, AIAA 2014-2897.
- <sup>14</sup>Goodwin, R.V., Fuleki, D., "Turbofan Ice Crystal Rollback Investigation and Preparations Leading to the Second, Heavily Instrumented, Ice Crystal Engine Test at NASA PSL-3 test Facility," submitted to 2016 AIAA Aviation. *8th AIAA Atmospheric and Space Environments Conference*, Washington, D.C, June 13-17, 2016, AIAA 2016.
- <sup>15</sup>Bencic, T.J., Fagan, A.F., Van Zante, J.F., Kirkegaard, J.P., Rohler, D.P., Maniyedath, A., and Izen, S.H., "Advanced Optical Diagnostics for Ice Crystal Cloud Measurements in the NASA Glenn Propulsion Systems Laboratory," *5th AIAA Atmospheric and Space Environments Conference*, AIAA 2013-2678, June 2013.
- <sup>16</sup>Bencic, T.J., "Aircraft engine icing instrumentation used in the NASA Glenn Propulsion Systems Laboratory," oral presentation submitted to 2016 AIAA Aviation. *8th AIAA Atmospheric and Space Environments Conference*, Washington, D.C, June 13-17, 2016
- <sup>17</sup>Fuleki, D.M., Mahallati, A., Knezevici, D.C., Currie, T.C., MacLeod, J.D., "Development of a Sensor for Total Temperature and Humidity Measurements under Mixed-Phase and Glaciated Icing Conditions," *6th AIAA Atmospheric and Space Environments Conference*. American Institute of Aeronautics and Astronautics, AIAA 2014-2751, June 2014.
- <sup>18</sup>Strapp, J.W., Chow, P., Maltby, M., Bezer, A.D., Korolev, A., Stomberg, I., and Hallet, J., "Cloud Microphysical Measurements in Thunderstorm Outflow Regions during Allied. BAe 1997 Flight Trials," *37th AIAA Aerospace Sciences Meeting and Exhibit*, Reno, NV, Jan 11-14, 1999, AIAA 99-0498.

<sup>19</sup> Strapp, J.W., Lilie, L.E., Emery, E.E., Miller, D., "Preliminary Comparison of Ice Water Content as Measured by Hot Wire Instruments of Varying Configuration.," *43<sup>rd</sup> AIAA Aerospace Sciences Meeting and Exhibit*, Reno, NV, Jan. 10-13, 2005, AIAA 2005-860.

<sup>20</sup>Walker, D.J., "Determination of engine recovery after an ice accretion rollback, engine performance deterioration and health monitoring using minimal instrumentation during icing testing at NASA Glenn PSL3," submitted to 2016 AIAA Aviation. *8th AIAA Atmospheric and Space Environments Conference*, Washington, D.C, June 13-17, 2016.

<sup>21</sup>Dischinger, D., Wolfgang, S.A., "Test Point Selection for Engine Crystal Icing Test at NASA PSL-3 for focused sensitivity, peak intensity, and anti-ice evaluations," oral presentation at 2016 AIAA Aviation. *8th AIAA Atmospheric and Space Environments Conference*, Washington, D.C, June 13-17, 2016.

<sup>22</sup>Tsao, J.C., and Struk, P.M., "NASA's Thought on Altitude Scaling for Engine Ice Crystal Icing.," Invited presentation in 2013 EIWG meeting, Hood River, OR, September 18, 2013.

<sup>23</sup>Tsao, J. C., Struk, P.M. and Oliver, M.J., "Possible Mechanisms for Turbofan Engine Ice Crystal Icing at High Altitude," *6th AIAA Atmospheric and Space Environments Conference*, Atlanta, GA, June 16-20, 2014, AIAA 2014-3044.